

Theoretical interpretation for $2p - nd$ absorption spectra of iron, nickel, and copper in X-ray range measured at the LULI2000 facility

M. Poirier^{1,a}, P. Arnault², S. Bastiani-Ceccotti³, T. Blenski¹,
F. de Gaufridy de Dortan⁴, F. Gilleron², G. Loisel^{1,3,5}, J.-C. Pain²,
Q. Porcherot², C. Reverdin², V. Silvert², F. Thais¹ and S. Turck-Chièze⁵

¹ CEA, IRAMIS, Service "Photons, Atomes et Molécules", Centre d'Études de Saclay, 91191 Gif-sur-Yvette, France

² CEA, DAM, DIF, 91297 Arpajon, France

³ LULI, UMR 7605 CNRS - École Polytechnique, 91128 Palaiseau, France

⁴ Institute of Nuclear Fusion, Universidad Politécnica de Madrid, Spain

⁵ CEA, IRFU, Service d'Astrophysique, Centre d'Études de Saclay, 91191 Gif-sur-Yvette, France

Abstract. The $2p - nd$ absorption structures in medium Z elements present a valuable benchmark for atomic models since they exhibit a complex dependence on temperature and density. For these transitions lying in the X-ray range, one observes a competition between the spin-orbit splitting and the broadening associated to the excitation of complex structures. Detailed opacity codes based on the HULLAC or FAC suites agree with the statistical code SCO; but in iron computations predict higher peak absorption than measured. An addition procedure on opacities calculated with detailed codes is proposed and successfully tested.

1. INTRODUCTION

The determination of accurate absorption spectra of warm dense matter in X-ray and extreme-UV (EUV) domains is essential for the radiative transfer properties of plasmas, the knowledge of which is required in various fields such as astrophysics, source development, or inertial fusion sciences [1, 2]. The study of the dependence of such structures with ion temperature T and mass density ρ provides useful information about the atomic structure of the involved ions. In this sense, Back *et al* [3] have demonstrated that in a germanium plasma, when the temperature T increases from 20 eV to 50 eV, the $2p - 3d$ array evolves from a spin-orbit split structure to a single structure. The recent experiment performed on the LULI2000 facility [4] aimed at checking a similar effect at fixed T but varying the atomic number Z : at $T \sim 20$ eV, the $2p - 3d$ splitting is expected to vanish when Z decreases from 29 (Cu) to 26 (Fe). To describe this experiment, several models have been used and compared [5]: a statistical analysis with the superconfiguration code SCO [6], detailed-level accounting approaches using either HULLAC [7] or FAC [8] packages, the mixed approach SCO-RCG [9] combining the SCO approach with a detailed line analysis based on Cowan's code, and the collisional-radiative code SCRIC [10] suited to characterize the non-local-thermodynamic-equilibrium effects. It turned out that HULLAC

^ae-mail: michel.poirier@cea.fr

Table 1. List of configurations used in HULLAC for $2p - nd$ opacity calculations. The closed shell core $1s^2 2s^2 3s^2$ is omitted. N is the total number of electrons. The numbers of holes in $3p$ subshell i and j depend on the case considered and are defined in the text.

Subset	Configurations
(a)	$2p^6 3p^{6-i} 3d^{N-18+i}$
(b)	$2p^5 3p^{6-i} 3d^{N-17+i}$
(c)	$2p^5 3p^{6-j} 3d^{N-18+j} 4d$

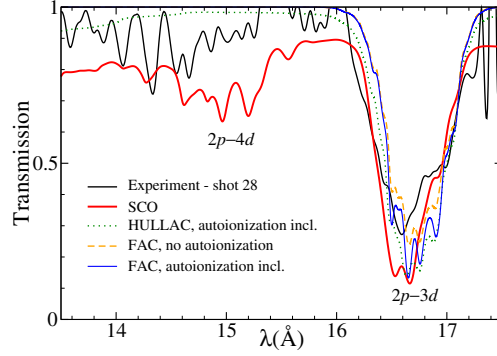


Figure 1. Transmission of an iron sample of areal mass $20 \mu\text{g}/\text{cm}^2$ in the X-ray range.

and FAC codes, while agreeing with other codes in the $2p - 3d$ region, were unable to deal with the description in the full analyzed range (8–18 Å) encompassing the $2p - nd$ transitions with $n > 3$. We propose here a method to deal with such higher terms using detailed codes. This will allow us to check in X-ray spectra the influence of configuration interaction (CI), keeping in mind that CI was shown to be essential in EUV xenon emission analysis [11].

2. COMPARISON OF EXPERIMENTAL RESULTS TO STATISTICAL AND DETAILED CODES

A presentation of the LULI campaign on X-ray opacities of iron, nickel, copper, and germanium, as well as details about the theoretical models used have been published elsewhere [4, 5].

In the *iron* case, it has been shown [5] that, ignoring the configurations with a $3p$ open subshell, the $2p - 3d$ structure at a temperature $T \sim 20 \text{ eV}$ as calculated by HULLAC is composed of well-separated components, in contradiction with the prediction from the SCO code and with the experiment. The list of configurations is given in Table 1. Only subsets (a) and (b) are included, with $i = 0, 1, 2$ for each charge state, which means that $2p - 4d$ transitions are not included; the number of electrons N varies from 21 to 16 (Fe^{5+} to Fe^{10+}). Though this set looks limited, accounting for these 6 nonrelativistic configurations in these 6 ions leads to a HULLAC spectrum consisting of not less than 1.96×10^6 lines. Indeed, detailed codes can hardly deal with a set of configurations like {(a), (b), (c)} accounting simultaneously for $2p - 3d$ and $2p - 4d$ transitions if full configuration interaction is accounted for.

Figure 1 summarizes conclusions about the X-ray absorption in iron. Calculations are done for plasma temperature $T = 22 \text{ eV}$ and mass density $\rho = 4 \text{ mg}/\text{cm}^3$. FAC and HULLAC spectra are convoluted with a Gaussian of FWHM $\delta\lambda$ such as $\lambda/\delta\lambda = 400$, in order to account for the experimental uncertainties. One must first notice that SCO code, accounting for a huge number of configurations and billions of lines, reasonably agrees with the detailed codes HULLAC and FAC as far as the $2p - 3d$ (around 16.6 Å) transmission level is involved. Some discrepancies are noticeable on the line shape and can be attributed to the presence of side components such as the $2p - 4s$ on the blue wing of the $2p - 3d$ structure, and to the approximate account for spin-orbit interaction in SCO. The parametric-potential codes HULLAC and FAC turn out to give similar absorption profiles. Besides, one must notice that in detailed codes such as FAC the line-broadening effects are essential: without accounting for autoionization, the transmission level on the center of the $2p - 3d$ structure would be significantly higher. Compared to experimental data, the computed transmission seems underestimated. The too

important absorption cannot be attributed to an insufficient complexity in the models: with more lines or more broadening effects included, the computed transmission would be even lower. A previous analysis [5] identified the most probable cause for this as being inhomogeneities in the sample temperature, density, or thickness.

The remaining significant discrepancy between HULLAC or FAC and SCO or experimental data concerns the 14–15 Å range where the higher transitions $2p - nd$, $n \geq 4$ are found. This limitation with detailed codes will be addressed and partially lifted in Sec. 3.

The $2p - nd$ X-ray opacity of *nickel* has been discussed in detail in Ref. [4, 5]. Let us mention here that the $2p - 3d$ splitting partially appears in the LULI data though less than expected. The correct ratio of the transmission on the two structures needs a thorough account for spin-orbit effects. Less inhomogeneity is inferred since the measured $2p - 3d$ absorption level is roughly as expected. A partial agreement is observed on higher $2p - nd$ structures.

Concerning the *copper* X-ray opacity, a previous SCO analysis [5] has shown that the $3p$ subshell opening is in the current conditions negligible ($\langle p_{3s} \rangle = 2$, $\langle p_{3p} \rangle = 5.93$). The $2p - 3d$ splitting shows up, but is less visible in LULI data than in computations from SCO or from detailed codes.

3. COMBINATION OF PARTIAL SPECTRA IN DETAILED CODES

The spectral opacity $\kappa(\lambda)$ is related to the transmission $\mathcal{T}(\lambda)$ by $\mathcal{T}(\lambda) = \exp(-\kappa(\lambda)\sigma)$, σ being the areal mass. Accounting for $2p - 3d$ and $2p - 4d$ structures simultaneously in an opacity calculation using a detailed code such as HULLAC may be too demanding in a full configuration interaction framework. We thus propose the following procedure. We first compute $2p - 3d$ opacity, with subsets of configurations (a) and (b) as listed in Table 1, the value of i being case-dependent. We then compute separately the $2p - 4d$ opacity with subsets {(a), (c)}. Next, we add these opacities to get the “combined” opacity. Finally, *when it is possible*, we compare this sum to the full “consistent” computation including simultaneously the subsets {(a), (b), (c)}.

This procedure has been applied to a copper plasma at $T = 20$ eV and $\rho = 5$ mg/cm³. According to the above-mentioned SCO prediction showing that $3p$ opening is negligible, the configurations used are those labeled (a), (b) and (c) in Table 1 with $i = j = 0$. The above addition procedure has been tested: it appears that the full consistent computation including $3d$ and $4d$ excitations (and therefore their possible interaction) is in fair agreement with the combined opacity as defined above, with the exception of the high wavelength region. There, one notices that the combined opacity is twice as large as the one from the full calculation. This discrepancy can be explained by a redundancy in the computation of combined opacity: because both groups used to compute $2p - 3d$ and $2p - 4d$ opacities include configurations in subset (a), the photoionization process $2p^6 3p^6 3d^{N-18} \rightarrow 2p^6 3p^6 3d^{N-19}$ is counted twice.

This redundancy can be eliminated by a simple screening of the atomic data used to compute, e.g., the $2p - 4d$ opacity: the transitions *inside* the subset (a) are canceled in this computation. As seen in Fig. 2, the $2p - 4d$ opacity does not include anymore the photoionization process $2p^6 [3]^{N-12} \rightarrow 2p^6 [3]^{N-13}$, which explains the absence of the background of $\sim 10^2$ cm²/g. But the combined opacity (green broken curve, addition of $2p - 3d$ and screened $2p - 4d$) is now in very good agreement with the full consistent computation. This validates the piecewise opacity-computation procedure proposed above. Additionally, this demonstrates that the interaction between configurations with a $3d$ and $4d$ excitation — included in the consistent computation, but ignored in the sum — is negligible in this energy domain.

In a similar way, the addition procedure has been tested for $2p - nd$ absorption in iron. A calculation of the transmission is shown in Fig. 3. This improves the agreement with SCO and experiment in the $2p - 4d$ region that was missing in Fig. 1.

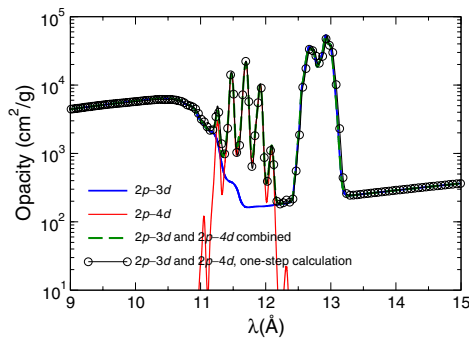


Figure 2. Opacity of a copper plasma at $T = 20\text{ eV}$ and $\rho = 5\text{ mg/cm}^3$ computed with HULLAC. The contribution of $2p - 3d$ and $2p - 4d$ transitions are shown separately. Redundancies have been eliminated in the $2p - 4d$ opacity computation. See text for details.

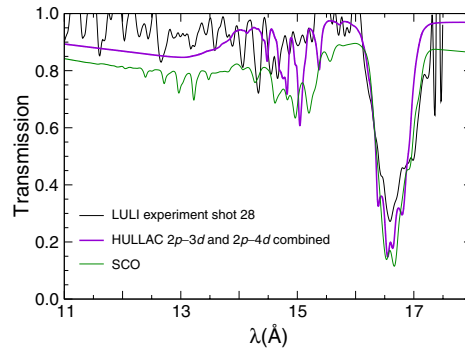


Figure 3. Transmission of an iron plasma. The thermodynamic parameters are those of Fig. 1. The LULI experimental data are compared to the statistical code SCO and to the present HULLAC results using the addition-of-opacity procedure.

4. CONCLUSION

Experiments on laser-plasma interactions such as those done on the LULI2000 facility provide a valuable benchmark for opacity codes. It has been shown here that inner subshell opening may give rise to complex structures which statistical codes can more easily track than detailed codes. When configurations weakly interact a procedure combining opacities from various transitions has been proposed and successfully checked. The data obtained from laser-plasma interaction are generally more complex to analyze than the recently published spectra from Z-pinch facilities [12]: because temperature is lower in laser experiments, the population in $3p$ subshell plays then a significant role. Finally the present analysis provides valuable information about M shell populations in conditions relevant to astrophysics; these data will be useful in forthcoming experiments on 3–3 transitions in the EUV domain.

This work has been partly supported by the European Communities under the contract of Association between EURATOM and CEA within the framework of the European Fusion Program.

References

- [1] T.S. Perry, K.S. Budil, R. Cauble, R.A. Ward, D.R. Bach, C.A. Iglesias, B.G. Wilson, J.K. Nash, C.C. Smith, J.M. Foster et al., *J. Quant. Spectrosc. Radiat. Transfer* **54**, 317 (1995)
- [2] C. Chenais-Popovics, *Laser Part. Beams* **20**, 291 (2002)
- [3] C.A. Back, T.S. Perry, D.R. Bach, B.G. Wilson, C.A. Iglesias, O.L. Landen, S.J. Davidson, B.J.B. Crowley, *J. Quant. Spectrosc. Radiat. Transfer* **58**, 415 (1997)
- [4] G. Loisel, P. Arnault, S. Bastiani-Ceccotti, T. Blenski, T. Caillaud, J. Fariaut, W. Fölsner, F. Gilleron, J.C. Pain, M. Poirier et al., *High Energy Density Phys.* **5**, 173 (2009)
- [5] T. Blenski, G. Loisel, M. Poirier, F. Thais, P. Arnault, T. Caillaud, J. Fariaut, F. Gilleron, J.C. Pain, Q. Porcherot et al., *Phys. Rev. E* **84**, 036407 (2011)
- [6] T. Blenski, A. Grimaldi, F. Perrot, *Phys. Rev. E* **55**, R4889 (1997)

IFSA 2011

- [7] A. Bar-Shalom, M. Klapisch, J. Oreg, *J. Quant. Spectrosc. Radiat. Transfer* **71**, 169 (2001)
- [8] M.F. Gu, *Astrophys. J.* **582**, 1241 (2003)
- [9] Q. Porcherot, J.C. Pain, F. Gilleron, T. Blenski, *High Energy Density Phys.* **7**, 234 (2011)
- [10] F. de Gaufridy de Dortan, *Tech. Rep. CEA-R-6115*, CEA (2006)
- [11] F. Gilleron, M. Poirier, T. Blenski, M. Schmidt, T. Ceccotti, *J. Appl. Phys.* **94**, 2086 (2003)
- [12] J.E. Bailey, G.A. Rochau, C.A. Iglesias, J. Abdallah, J.J. MacFarlane, I. Golovkin, P. Wang, R.C. Mancini, P.W. Lake, T.C. Moore et al., *Phys. Rev. Lett.* **99**, 265002 (2007)